Calibration of Radiation Codes Used in Climate Models: Comparison of Clear-Sky Calculations with Observations from the Spectral Radiation Experiment and the Atmospheric Radiation Measurement Program

R. G. Ellingson, S. Shen, and J. Warner
University of Maryland
College Park, Maryland

Background

The InterComparison of Radiation Codes in Climate Models (ICRCCM) showed large differences between model calculations of longwave fluxes and heating rates—even for clear-sky conditions (Luther et al. 1988). The discrepancies could not be resolved with either pyrgeometer measurements or line-by-line calculations because

- Pyrgeometer errors are the magnitude of the discrepancies.

- Uncertainties in the physics of line wings and in the proper treatment of the continuum make it impossible for line-by-line models to provide an absolute reference.

The 1984 and 1988 ICRCCM Workshops called for a detailed spectral radiation experiment to resolve the discrepancies. The Spectral Radiation Experiment (SPECTRE) and, eventually, the Atmospheric Radiation Measurement (ARM) Program arose in part as a result of these recommendations.

Objectives and Approach

The long-term objectives of our study are to

- Determine the range of agreement between longwave observations and model calculations ranging from line-by-line models to those used in climate models.

- Understand the causes for the differences between calculations and observations.

- Develop improved parameterizations for use in climate models.

The approach that we plan to follow is to

- Compare model calculations with measurements of the zenith infrared radiance spectra obtained by the Atmospherically Emitted Radiance Interferometer (AERI) and pyrgeometers (when appropriate).

- Change model parameterizations on the basis of discrepancies with observations and new physical insight.

This paper summarizes preliminary results obtained from the comparisons of calculations made by different models with observations obtained during the SPECTRE and ARM. The study is limited at this time to clear-sky conditions because we believe it is necessary to ascertain the performance of radiation models under these conditions in order to more fully understand observations made under more general cloudy conditions.

Calculations and Observations

This study uses calculations from line-by-line, narrow-band and broad-band radiation codes using identical meteorological sounding data as input. All line-by-line calculations shown herein were done with the code line-by-line radiative transfer model (LBLRTM), version 3.2, continuum version 2.4, using the 92'HITRAN line database.

Note that LBLRTM is a refinement of FASCODE3 (Clough et al. 1989).[a]

The narrow-band model calculations were performed with the codes LOWTRAN7 (Kneizys 1988), MODTRAN2, Ellingson (Ellingson and Serafino 1984; Ellingson et al. 1994). The broad-band calculations were carried out with codes used in different climate models including Colorado State University (Harshvardhan and Corsetti 1984), European Center for Medium Range Weather forecasting (Morcrette 1991), National Meteorological Center (NMC; Schwarzkopf and Fels 1991), Community Climate Model (Kiehl et al. 1987) and the Canadian Climate Center[a].

All of the radiation codes include effects of H_2O, CO_2 and O_3, although with different parameterizations. The LBLRTM and narrow-band calculations also include the effects of CH_4 and N_2O. The LBLRTM calculations also include the effects of other trace gases including F10 and F11 and CCl4. Note that climatological concentrations of CO_2, CH_4, N_2O, F10, F11 and CCl4 are used throughout. Ozone concentrations are specified by the appropriate climatological profile for calculations compared with ARM spectra, whereas ozonesonde data are used for the SPECTRE comparisons.

The temperature profiles used in the models were specified from radiosonde soundings launched within 15 min (ARM) or 30 min (SPECTRE) of an observed spectra. The water vapor profiles were specified from the radiosonde observations for comparisons made with ARM data, whereas Raman lidar observations were used to specify the water vapor profiles for the comparisons with SPECTRE spectra.

All comparisons of spectral radiance shown herein use observations from the AERI which is deployed at the CART site. Note that this is the same instrument that was deployed during SPECTRE. AERI radiance data in the most opaque portion of the 15μm CO_2 band system are used to specify the near-environment temperature in the radiation model calculations.

Selection of 'Clear-Sky' Periods

The selection of periods of clear skies was relatively straightforward for SPECTRE since we had copious

observer logs, and we had Raman lidar data to use to note the presence of clouds. In all, 26 cases were found with clear skies and spectra within 30 min of a radiosonde launch and a Raman lidar sounding. All are were from nighttime periods.

The ARM data sets to date do not provide adequate information to ascertain cloud conditions during the periods of AERI observations near the time of radiosonde launch. As a result, we screened the ARM data set according to a variety of rather arbitrary conditions to select a set of data that we believe to be the clearest of all the ARM AERI observing periods.

The cloud-screening procedure was done in the following fashion. First, surface observations and AERI data were examined for periods when clear or partly cloudy conditions were observed within 15 min of a radiosonde launch. The AERI spectra within these periods were sorted according to the difference between the blackbody temperatures in the most opaque (15μm) and the 10μm regions (ΔT_{1s}). We arbitrarily specified that 'clear' conditions might occur when $\Delta T_{1s} > 50°C$ and 30°C and for the months of November through April and May through October, respectively. Finally, the difference between the blackbody temperatures in the 15μm region and the 4μm window (denoted ΔT_{2s}) were used to further stratify the data. Model calculations showed $\Delta T_{2s} > 46°C$ for all ARM cases. To allow for possible systematic errors, we specified that 'clear' conditions occur when $\Delta T_{2s} > 40°C$.

The distributions of ΔT_{2s} for ARM and SPECTRE are shown in Figure 1. Note that we had not examined the values for SPECTRE before we examined the ARM data. The SPECTRE results in Figure 1 show a much closer agreement between the observed and calculated values than those observed so far in ARM. Furthermore, the observed values of ΔT_{2s} tend to be lower in SPECTRE than in ARM. This result could be due to a variety of causes, but the most obvious is scattering of solar radiation into the AERI field of view during ARM. All SPECTRE cases were at night, whereas the ARM spectra were primarily during daylight. Increased scattering, as well as increased thermal emission in the 4μm region, is expected in the presence of clouds, resulting in relatively small values of ΔT_{2s}. As cloud data from the various lidars become available, it may be possible to design more precise cloud detection criteria for the AERI.

(a) Available from S. A. Clough, Atmospheric and Environmental Research, Inc., Boston, Massachusetts.
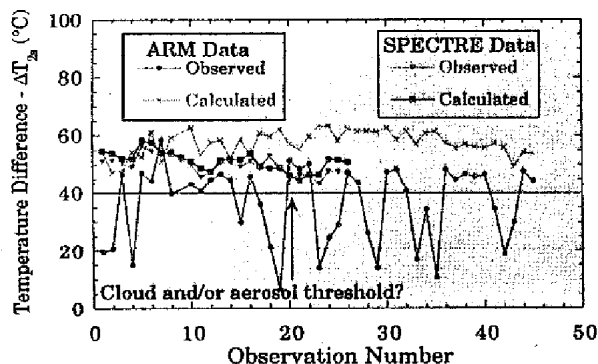
Figure 1. Distributions of DT2s for SPECTRE and ARM data. ΔT_{2s} = blackbody temperature at 675 cm^{-1} blackbody temperature at 2510 cm^{-1}.

Comparisons of Observations with Calculations

Shown in Figure 2 are a) the mean observed spectrum of downwelling radiance for the 26 clear-sky SPECTRE cases, and b) the spectra of the mean and rms observed-LBLRTM radiances (ΔRad). In general, the SPECTRE comparisons show mean and rms agreement between the observed and calculated radiances to within the accuracy of the observations (about 1% full scale). The major discrepancies occur in the region of the 9.6µm O$_3$ band.

Figure 3 shows the spectra of the mean and rms ΔRad for the 'clear-sky' ARM data for different periods. The figure clearly shows that in the 800 to 1250 cm^{-1} window region, observed radiances are greater than calculated. The differences are larger than those found during SPECTRE, and they are seasonally varying.

If the parameterization for the water vapor continuum absorption in the 8µm to 12µm region were incorrect, ΔRad and the total precipitable water (PW) should show a marked correlation. Figure 4 shows the dependence of the spectrally integrated ΔRad for the 800-1250 cm^{-1} window region (sans O$_3$) for ARM and SPECTRE data. Both data sets show a marked, but different, correlation of the differences on total PW. Both sets of results are consistent with an underestimated continuum absorption and/or a dependence of aerosol loading on precipitable water. However, the large discrepancy between the SPECTRE

and ARM results points to the possibility of the absence of true low aerosol, 'clear-skies' during ARM to date and/or errors in the humidity measurements.

The AERI and SPECTRE results lead to significant differences in model **flux** uncertainties at high amounts of water vapor. Our calculations show the ARM and SPECTRE downward flux uncertainties to be about 15 and 5 W m^{-2} for PW > 4 cm, respectively. Differences of the order of 5 W m^{-2} are close to the magnitude acceptable to many energy budget studies, whereas the values estimated from the ARM data would indicate that the model calculations are unacceptable. Obviously, similar comparisons need to be done with more precise specification of the cloud and/or aerosol conditions.

In Figure 5, SPECTRE AERI radiances in the 800 to 1250 cm^{-1} region are compared with calculations from different models using identical input data. Several models systematically underestimate the radiance in this interval, although each explains about the same variance. Note that a difference of 2 in radiance units in this interval translates to a flux difference of about 4 W m^{-2}.

In Figure 6, fluxes inferred from the SPECTRE AERI data are compared with those calculated by different climate model radiation codes. Note that the AERI 'flux' was determined using LBLRTM calculations for the spectral interval not observed and by assuming that LBLRTM gives the correct angular dependence in the observed interval. For comparison purposes, the mean and rms differences between the AERI and LBLRTM fluxes are 2.5 and 3.1 W m^{-2}, respectively. With the exception of the NMC model, the other models tend to underestimate the observed flux, some by as much as 15 W m^{-2}. Only about one-third of the flux differences can be accounted for by the underestimates in the 800 to 1250 cm^{-1} region.

Conclusions

Our analyses to date lead to the following conclusions:

- Calculations with LBLRTM show excellent agreement with clear-sky AERI observations from SPECTRE, although there is a trend of increasing differences with increasing precipitable water vapor.

- Similar comparisons made with ARM data show poorer agreement. The reasons for these differences are likely
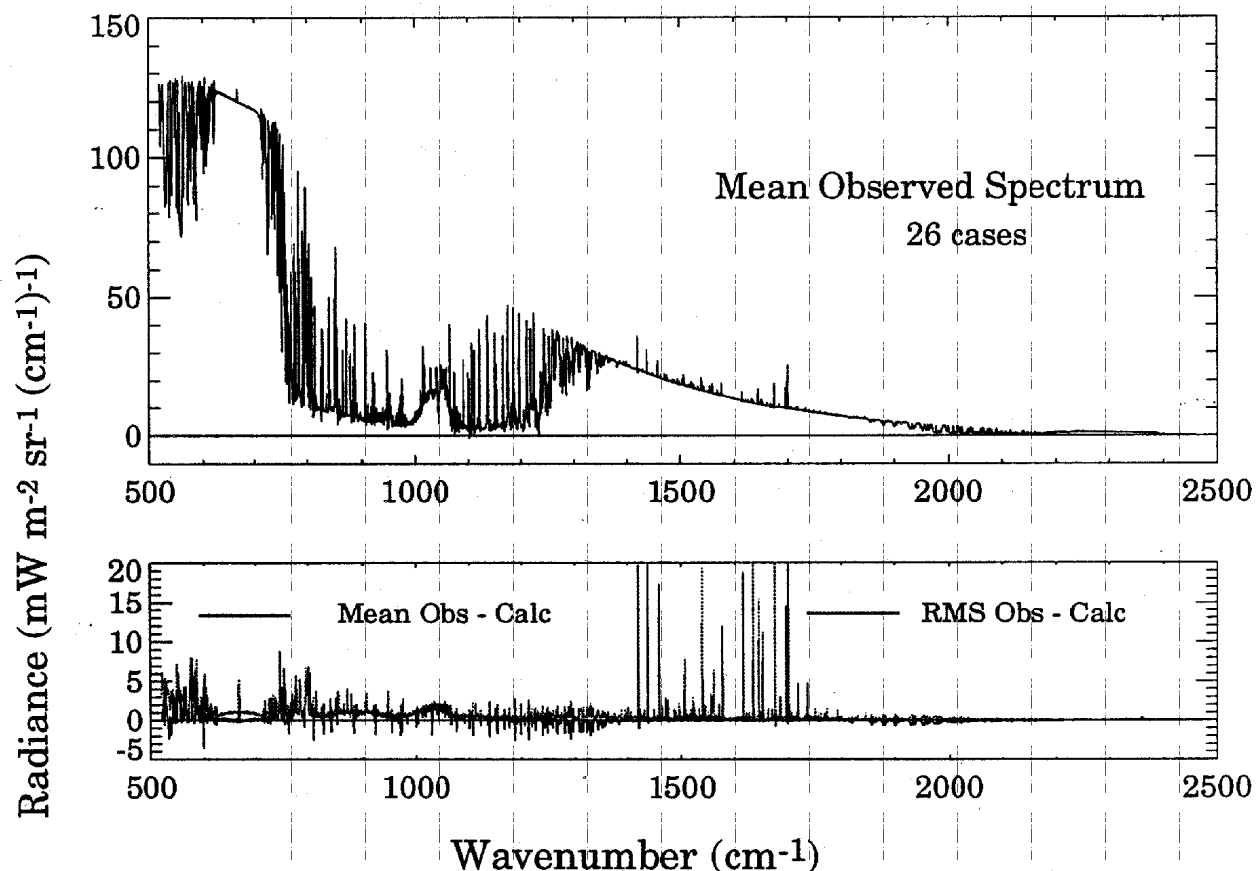
Figure 2. Mean observed spectrum and mean and rms AERI-LBLRTM spectra for SPECTRE clear days.

related to the difficulty with defining clear-sky conditions and/or aerosols. These difficulties should diminish as cloud-sensing lidars become operational.

- The SPECTRE data show that one climate model code (NMC) reproduces the AERI data and LBLRTM results to better than 5 W m^{-2} rms over the range of 200 to 300 W m^{-2}.

- Several parameterizations significantly underestimate the AERI flux, some by more than 15 W m^{-2}~ ±5%. However, all the models explain about the same observed variance ~ 99%.

- The AERI-Model differences in the 8µm to 12 µm region account for only about 30% of the total flux differences.

We tentatively attribute the additional flux differences to improper treatment of overlap between H_2O and CO_2 and/or the treatment of the more strongly absorbing regions of H_2O and CO_2.

References

Clough, S. A., F. X. Kneizys, G. P. Anderson, E. P. Shettle, J. H. Chetwynd, L. W. Abreu, L. A. Hall, and R. D. Worsham. 1989. FASCOD3 - Spectral simulation. IRS '88: *Current Problems in Atmospheric Radiation*, J. Lenoble and J.-F. Geleyn, eds., pp. 372-375. A. Deepak Publishing, Hampton, Virginia.
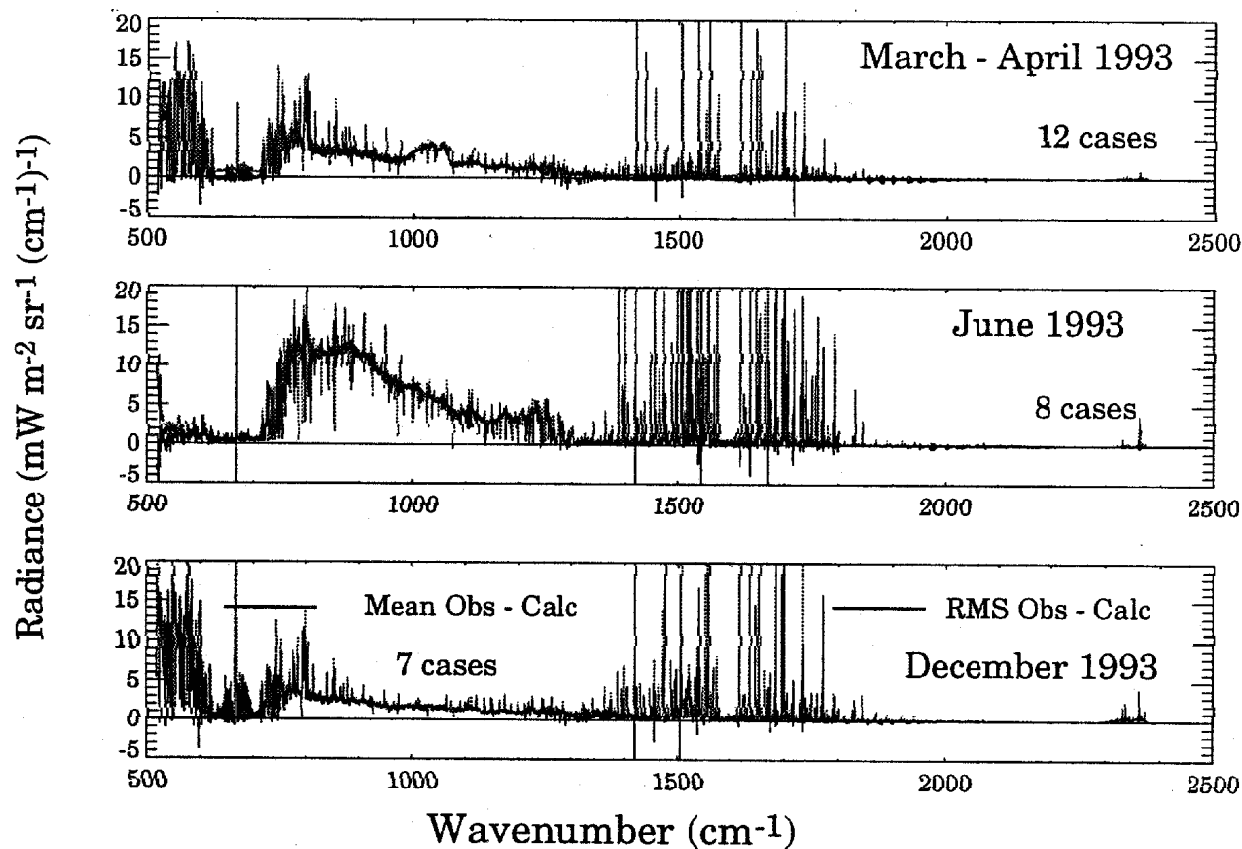
Figure 3. Mean and rms AERI-LBLRTM spectra for ARM clear days.
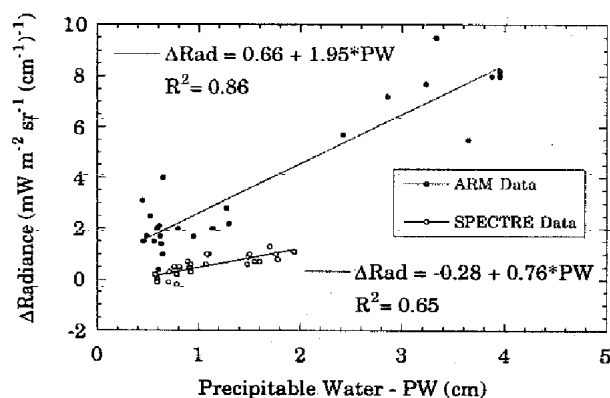

Figure 4. AERI Observed—LBLRTM radiance in the 800-900 + 1110-1250 cm^{-1} interval.

Ellingson, R. G., and G. N. Serafino. 1984. Observations and calculations of aerosol heating over the Arabian Sea during MONEX. *J. Atmos. Sci.* **41**:575-589.

Ellingson, R. G., H-T. Lee, D. Yanuk, and A. Gruber. 1991. Validation of a technique for estimating outgoing longwave radiation from HIRS radiance observations. *J. Atmos. Ocean. Tech.,* **11**:357-365.

Harshvardhan, and T. G. Corsetti. 1984. *Longwave radiation parameterization for the UCLA/GLAS GCM.* NASA-TM-86072. NASA, Greenbelt, Maryland.

Kiehl, J. T., et al. 1987. *Documentation of radiation and cloud routines in the NCAR Community Climate Model (CCM1).* NCAR/TM-288+IA, National Center for Atmospheric Research, Boulder, Colorado.
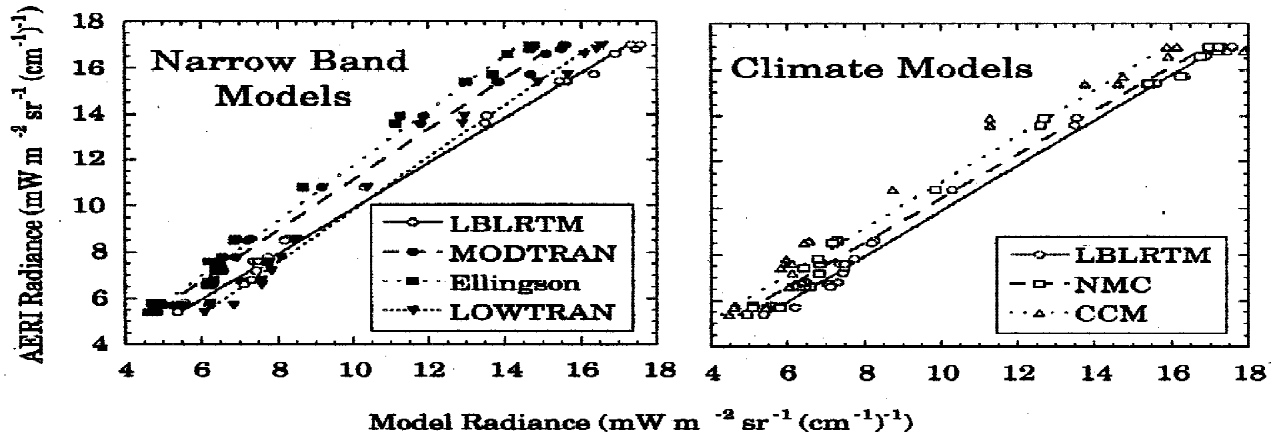
Figure 5. Comparison of AERI and model radiances for the 800-1250 cm^{-1} interval.
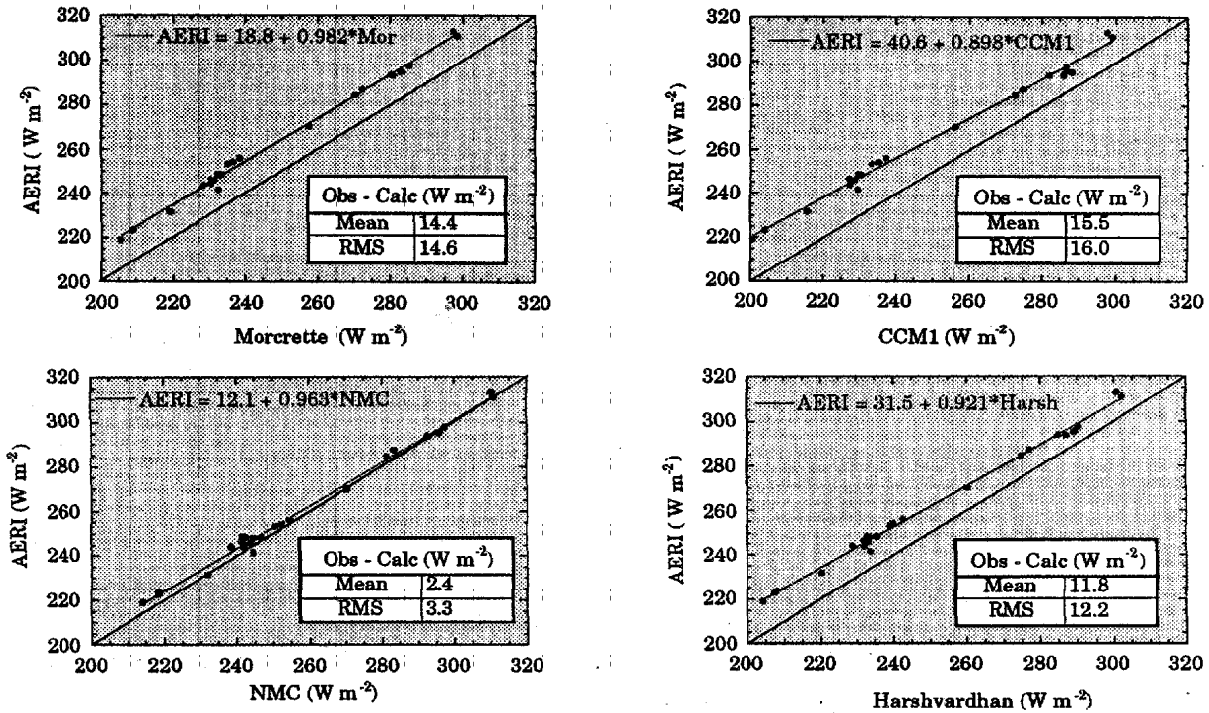

Figure 6. Comparison of different climate model flux calculations with AERI (SPECTRE) fluxes.

Working Group Reports

Kneizys, F. X., E. P. Shettle, L. W. Abreu, J. H. Chetwynd, G. P. Anderson, W. O. Gallery, J.E.A. Selby, and S. A. Clough. 1988. *Users Guide to LOWTRAN 7.* AFGL-TR-88-0177, Air Force Geophysics Laboratory, Hanscom AFB, Massachusetts.

Luther, F. M., R. G. Ellingson, Y. Fouquart, S. Fels, N. A. Scott, and W. Wiscombe. 1988. Intercomparison of radiation codes in climate models (ICRCCM): Longwave clear-sky results - A workshop summary. *Bull. Am. Met. Soc.* **69**:40-48.

Morcrette, J.-J. 1991. Radiation and cloud radiative properties in the European Center for Medium Range Weather Forecasts forecasting system. *J. Geophys. Res.* **96**:9121-9132.

Schwarzkopf, M. D., and S. B. Fels. 1991. The simplified exchange method revisited: An accurate, rapid method for computation of infrared cooling rates and fluxes. *J. Geophys. Res.* **96**:9075-9096.